



FTIR STUDIES OF PLASTICIZED PVC DOPED WITH $\text{NH}_4\text{CF}_3\text{SO}_3$ POLYMER ELECTROLYTE MEMBRANE

Siti Khatijah Deraman¹, Ri Hanum Yahaya Subban^{2,3} and Nor Sabirin Mohamed⁴

¹Faculty of Applied Sciences, Universiti Teknologi MARA, Tapah, Perak, Malaysia

²Faculty of Applied Sciences, Universiti Teknologi MARA, Shah Alam, Selangor, Malaysia

³Institute of Science, Universiti Teknologi MARA, Shah Alam, Selangor, Malaysia

⁴Center for Foundation Studies in Science, University of Malaya, Kuala Lumpur, Malaysia

E-Mail: sitik1297@perak.uitm.edu.my

ABSTRACT

Fourier transform infrared (FTIR) spectroscopy studies of poly (vinyl) chloride (PVC), doped with ammonium trifluoro methane sulfonate ($\text{NH}_4\text{CF}_3\text{SO}_3$) salt and ionic liquid (IL) butyltrimethyl ammonium bis(trifluoromethyl sulfonyl) imide ($\text{Bu}_3\text{MeNTf}_2\text{N}$) were synthesized via solution cast technique. About 50 ml of tetrahydrofuran (THF) was used as the solvent. Interaction between the polymer, salt and ionic liquid ($\text{Bu}_3\text{MeNTf}_2\text{N}$) was confirmed by FTIR spectroscopy. FTIR spectra revealed that $\text{Bu}_3\text{MeNTf}_2\text{N}$ has weak interaction which suggesting that it acts mainly as a lubricant to facilitate polymer segmental motion.

Keywords: FTIR, ionic liquid, proton conductor, ammonium Trifluoromethanesulfonate.

INTRODUCTION

In recent years, electrically conducting polymers have attracted considerable attention in flexible electronic technology such as solar cells, organic light-emitting diodes (OLEDs), touch screens and flexible displays [1]. Electrically conducting polymers like polyaniline (PAN), polypyrrole (PPY) and polythiophene (PTH) are of great interest as new class of materials in industry during the last two decades, owing to their unique combination of characteristics: electronic, optical, magnetic properties and processing advantage of polymers [2]. Poly (vinylchloride) (PVC) is an outstanding membrane material because of its stiffness, low cost, excellent physical and chemical properties, acids, alkalis and solvent resistance, as well as mechanical properties [3]. Solid polymer electrolytes are an alternative to liquid combustible systems because they possess superior voltage, temperature and mechanical stability. These benefits though come with a large trade off with conductivity [4-5]. Poly(ethylene oxide) (PEO) has conductivity problems at ambient temperatures because of its semi-crystalline nature. Thus, it has become a research focus to energetically favored the amorphous phase by the inclusion of a secondary block copolymer [6], lower molecular weight polymers [7], ceramic particles [8,9], carbonate solvents [10] or ionic liquids (ILs) [11-13]. ILs are attractive additives because they are tunable systems that possess wide temperature and voltage stability, while having an appreciable conductivity without compromising safety.

Ionic liquids based on the imidazolium cations possess generally favorable properties and useful information gathered on them is easily accessible. They have many desirable properties such as low viscosity, wide electrochemical stability window and high conductivity [14]. Due to their favorable characteristics, ILs have also been used as an alternative to plasticizers which suffer from flammability, volatility and mechanical, electrochemical and thermal instability [15]. One of the

imidazolium cation based ionic liquids has been used in polymer electrolytes by many groups of researchers [16,17] since it is one of the least viscous ILs [18] and has potential uses in device applications [19,20].

In [11] have shown that adding 1-butyl-1-methyl pyrrolidinium to PEO results in a marked increase in ionic conductivity between 1 and 2 orders of magnitude. However, the upper limit of conductivity achievable in the polymer electrolyte is still one order less than the conductivity of the neat ionic liquid. Additionally the large ratio of ionic liquid to polymer in Shin's optimized electrolyte has adverse effects upon the transference number, inherently limiting the capacity that can be delivered by lithium with each cycle [21,22]. This led to interest in novel IL scaffolds that would overcome these observed limitations while mimicking the preferred method of Li^+ conduction through the polymer chains [23,24]. Research into sulfur and phosphorous based systems has demonstrated superior electrochemical stability and conductivity values relative to nitrogen based architecture [25,26].

In this work, the incorporation of ionic liquid $\text{Bu}_3\text{MeNTf}_2\text{N}$ increase conductivity of polymer electrolytes by imparting salt solvating power and high ion mobility. However, the drawback is the decrease in mechanical strength of the electrolyte [27]. Interaction of IL butyltrimethyl ammonium bis(trifluoromethyl sulfonyl) imide ($\text{Bu}_3\text{MeNTf}_2\text{N}$) as a plasticizer has been investigated by [28] using infrared spectroscopy. To further discuss the phenomena such as polymer-salt-plasticizer complexation, ion aggregation formation and interaction between the salt and plasticizer in the sample, Fourier transform infrared (FTIR) was employed. This paper reports some details of interactions between polymer-salt-plasticizer, polymer-plasticizer and salt-plasticizer.



EXPERIMENTAL

Poly (vinyl) chloride (PVC) with molecular weight of 2.33×10^5 gmol⁻¹, NH₄CF₃SO₃ (Sigma- Aldrich, 99.0 %), and Bu₃MeNTf₂N (Butyltrimethyl ammonium bis (trifluoromethyl sulfonyl) imide) ionic liquid (Sigma- Aldrich, 98.0 %) were used in this work. All chemicals were used as received. PVC and NH₄CF₃SO₃ were mixed with Bu₃MeNTf₂N in various wt.% ratio with a ratio of PVC- NH₄CF₃SO₃ fixed in 70:30 wt. %. Solution cast films were obtained by pouring the solution into glass petri dishes, which were dried at room temperature. The films

formed were further dried in a vacuum oven at 313 K for 24 hours. FTIR measurements were carried out using a Perkin-Elmer FTIR spectrometer with a resolution of 4 cm⁻¹ in transmittance mode from wave numbers 400 cm⁻¹ to 4000 cm⁻¹. Confirmation of complexation and the proposition of the conduction mechanism of the charge carriers were the objectives of performing FTIR spectroscopy. Table-1 lists the composition of these samples together with their sample name.

Table-1. Composition of PVC-NH₄CF₃SO₃-Bu₃MeNTf₂N polymer electrolytes.

Sample Name	PVC - NH ₄ CF ₃ SO ₃ [A4] (g)	Bu ₃ MeNTf ₂ N(g)	Bu ₃ MeNTf ₂ N(wt. %)
C1	1.4286	0.0752	0.50
C2	1.4286	0.1587	0.10
C3	1.4286	0.2521	0.15
C4	1.4286	0.3572	0.20
C5	1.4286	0.4762	0.25

RESULTS AND DISCUSSION

FTIR spectra of PVC-NH₄CF₃SO₃-Bu₃MeNTf₂N system

Figure-1(i) (a)-(i) shows the infrared spectra of the PVC-NH₄CF₃SO₃-Bu₃MeNTf₂N system in the region between 550 to 800 cm⁻¹. It is observed that addition of Bu₃MeNTf₂N to PVC-NH₄CF₃SO₃ did not cause much changes to the spectra until the concentration of Bu₃MeNTf₂N reaches 10 wt. % where a new peak is observed at 749 cm⁻¹. This peak increases in intensity as concentration of Bu₃MeNTf₂N increases and shifted to 748 cm⁻¹ when Bu₃MeNTf₂N concentration reaches 25 wt. %. This new peak may be attributed to the peak of Bu₃MeNTf₂N at 740 cm⁻¹ due to S-N stretching of Bu₃MeNTf₂N. Since there is hardly any noticeable changes in peaks of Bu₃MeNTf₂N plasticized PVC-NH₄CF₃SO₃ spectra, it can be inferred that the PVC-NH₄CF₃SO₃-Bu₃MeNTf₂N system is a mixed phase system with weak interaction.

Figure-1(ii) (a)-(i) shows the same set of spectra in the vicinity of the S-N-S asymmetric stretching mode of Bu₃MeNTf₂N at 1052 cm⁻¹. It can be observed that the spectra of Bu₃MeNTf₂N incorporated PVC-NH₄CF₃SO₃ complex looks much like that of the A4. The peak observed at 1068 cm⁻¹ in C1 have shifted from 1082 cm⁻¹ in A4 when 5 wt. % of Bu₃MeNTf₂N is added to PVC-NH₄CF₃SO₃. This peak increases in intensity as concentration of Bu₃MeNTf₂N increases indicating that the Bu₃MeNTf₂N has interacted with PVC-NH₄CF₃SO₃. The peak due to the salt at 1028 cm⁻¹ which is found at 1032 cm⁻¹ in A4 still persists, but has shifted to 1036 cm⁻¹ in the spectra of PVC-NH₄CF₃SO₃-Bu₃MeNTf₂N. It is also observed that the intensity of this

peak increases as Bu₃MeNTf₂N concentration increases. The assignment of this band to 'free' ions indicates that there exists a substantial concentration of 'free' triflate ions in the polymer complex. The increase in the intensity of this band implies an increase in the number of free ions from the addition of Bu₃MeNTf₂N. This could explain why conductivity increases upon addition of Bu₃MeNTf₂N as a result of greater dissociation of salt. Similar persistence in shape is observed for the peaks attributed to PVC-NH₄CF₃SO₃ at 1175 cm⁻¹ and 1236 cm⁻¹, which indicating that the Bu₃MeNTf₂N addition did not cause much noticeable changes in the spectra of PVC-NH₄CF₃SO₃. New peak is recorded at 1144 cm⁻¹ when 10 wt. % of Bu₃MeNTf₂N (C2) is added to PVC-NH₄CF₃SO₃. This new peak increases in intensity as the concentration of Bu₃MeNTf₂N increases. This peak may be attributed to the peak of Bu₃MeNTf₂N at 1132 cm⁻¹. Apart from that, the peak attributed to NH₄ bending at 1446 cm⁻¹ in A4 is shifted to lower wavenumber at 1435 cm⁻¹ upon incorporation of 15 wt. % Bu₃MeNTf₂N (C3) into PVC-NH₄CF₃SO₃.

For the band at 1347 cm⁻¹ of Bu₃MeNTf₂N, it is shifted to a higher wavenumber at 1361 cm⁻¹ for C3, inferring high SO₂⁻ aggregation. The substantial increase in the intensity of this peak as concentration of Bu₃MeNTf₂N increases is attributed to the lowering of the viscosity of the sample. This means that there are several factors which could contribute to increase in conductivity of Bu₃MeNTf₂N incorporated PVC-NH₄CF₃SO₃ complex. Firstly increase in the number of free ions as evidenced by the changes in intensity of the peak at 1032 cm⁻¹, and secondly the lowering of the viscosity of this complex as evidenced by the transformation of the peak at 1347 cm⁻¹.

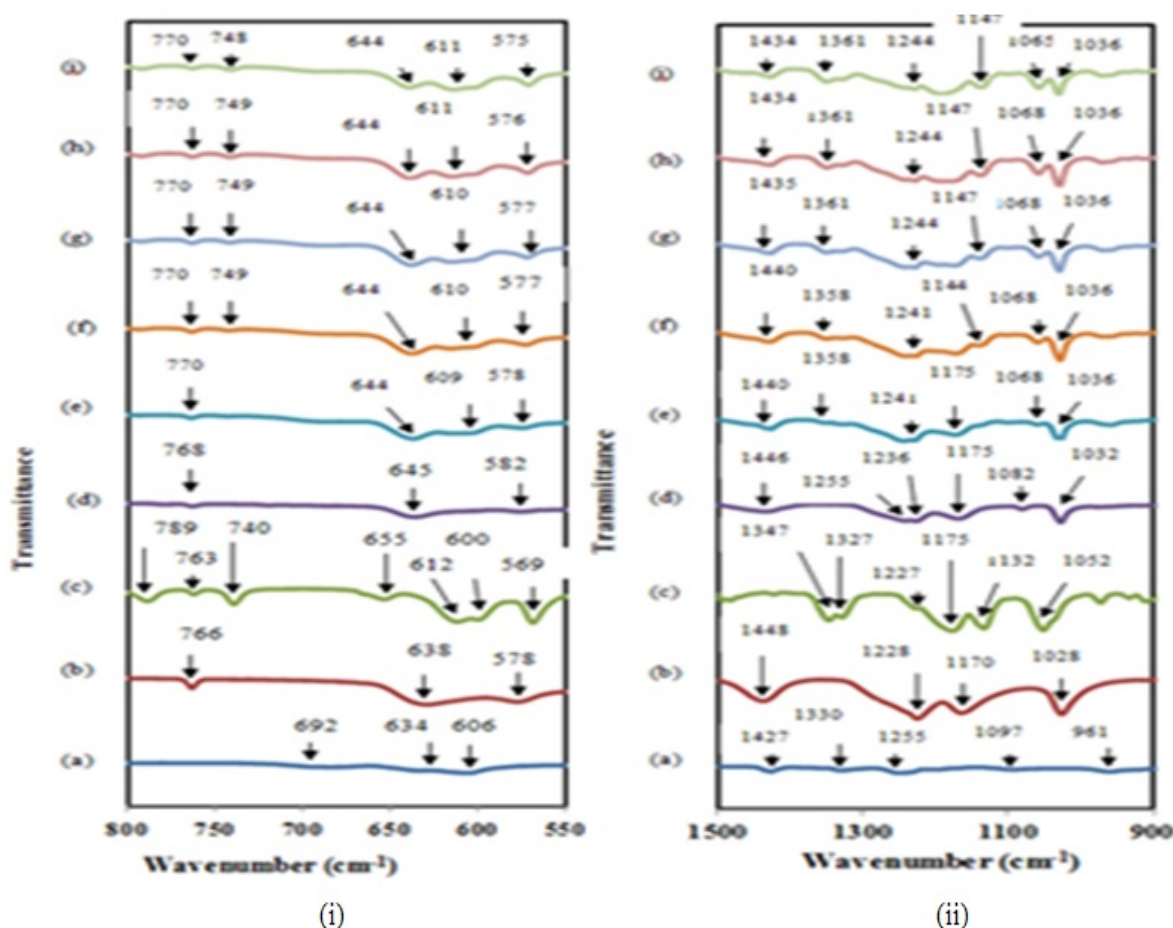


Figure-1. Infrared spectrum of (a) Pure PVC, (b) Pure $\text{NH}_4\text{CF}_3\text{SO}_3$, (c) Pure $\text{Bu}_3\text{MeNTf}_2\text{N}$, (d) A4, (e) C1, (f) C2, (g) C3, (h) C4 and (i) C5 Between 550 to 800 cm^{-1} region (ii) Between 900 to 1500 cm^{-1} region.

FTIR spectra of PVC- $\text{Bu}_3\text{MeNTf}_2\text{N}$ system

Figure-2 (a)-(e) shows the infrared spectra of the PVC- $\text{Bu}_3\text{MeNTf}_2\text{N}$ system in the region of 550-850 cm^{-1} . In this region, IR bands of PVC exist at 606, 634 and 692 cm^{-1} . When PVC is added to the $\text{Bu}_3\text{MeNTf}_2\text{N}$, all these peaks have disappeared. Vibrational bands attributed to $\text{Bu}_3\text{MeNTf}_2\text{N}$ are found at 569, 600, 612, 655, 740, 763 and 789 cm^{-1} . When PVC is added to the $\text{Bu}_3\text{MeNTf}_2\text{N}$, the characteristic peaks of $\text{Bu}_3\text{MeNTf}_2\text{N}$ at 569, 600, 612 and 655 cm^{-1} persist throughout the spectrum with slight shifts in wavenumbers even when the concentration of $\text{Bu}_3\text{MeNTf}_2\text{N}$ is 20 wt. %. It indicates that there is some interaction between the PVC and the $\text{Bu}_3\text{MeNTf}_2\text{N}$. This is further indicated by the change in shape of the spectra in the region of 600 to 655 cm^{-1} when PVC concentration is high.

Figure-3(a)-(e) shows the same set of spectra in the vicinity of S-N-S asymmetric stretching mode of the $\text{Bu}_3\text{MeNTf}_2\text{N}$ at 1052 cm^{-1} . This band exhibited an upward shift to 1058 cm^{-1} in PVC- $\text{Bu}_3\text{MeNTf}_2\text{N}$ complex

as the concentration of the $\text{Bu}_3\text{MeNTf}_2\text{N}$ increases. The similar upward shift is exhibited by the band at 1347 cm^{-1} indicating SO_2^- aggregation. Upward shifts were also observed for the bands at 1132, 1175, 1227 and 1468 cm^{-1} . The peaks attributed to PVC at 1097, 1330 and 1427 cm^{-1} have been obscured by the peaks at 1052, 1347 and 1468 cm^{-1} respectively while those at 1255 cm^{-1} have disappeared. The interaction between the PVC and the $\text{Bu}_3\text{MeNTf}_2\text{N}$ in this region mostly involved upward shifts of most bands of the $\text{Bu}_3\text{MeNTf}_2\text{N}$ and the disappearance of PVC peaks. A weak peak which is assigned as C-Cl stretching mode of PVC is shifted from 634 cm^{-1} and disappeared which indicates the interaction of PVC and $\text{Bu}_3\text{MeNTf}_2\text{N}$. Not much changes in the shape of the spectra occur in the region from 1400-1500 cm^{-1} when PVC concentration is high. The interaction between PVC and $\text{Bu}_3\text{MeNTf}_2\text{N}$ may be represented as shown in Figure-4.



www.arpnjournals.com

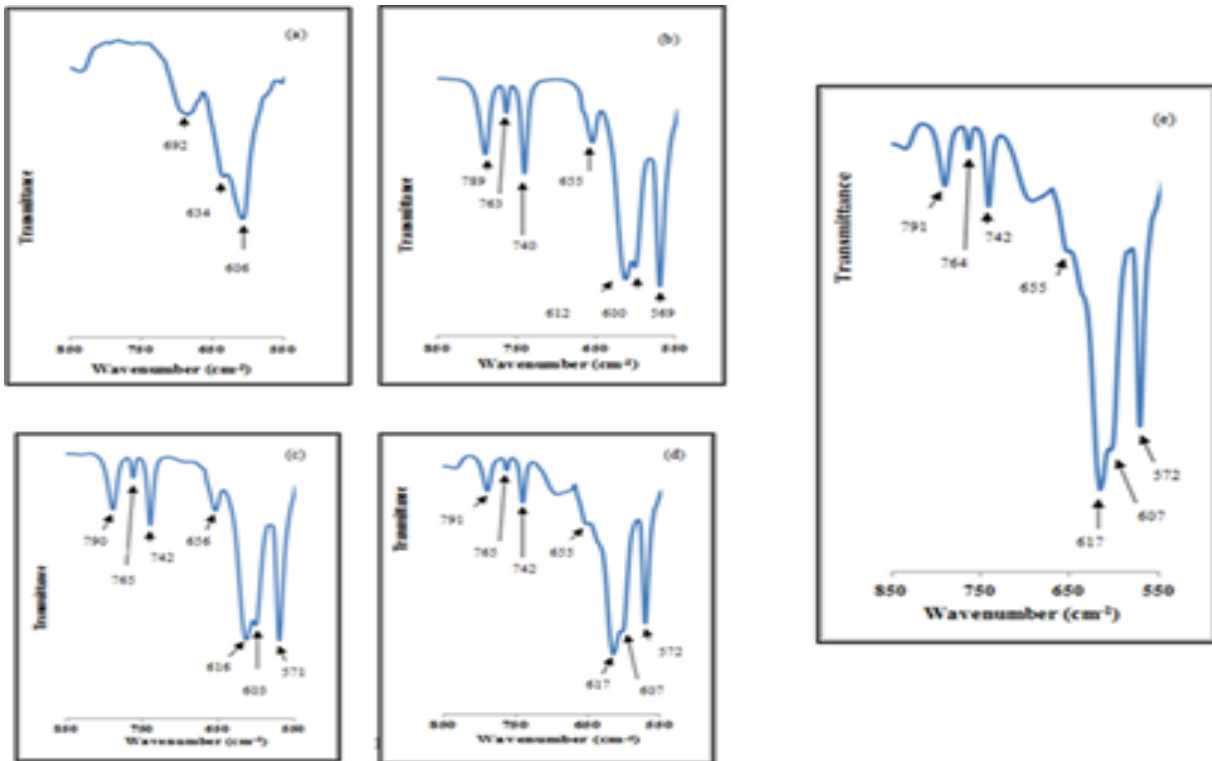


Figure-2. Infrared spectrum of (a) Pure PVC, (b) Pure $\text{Bu}_3\text{MeNTf}_2\text{N}$, (c) 20 wt. % PVC-80 wt. % $\text{Bu}_3\text{MeNTf}_2\text{N}$, (d) 50 wt. % PVC -50 wt. % $\text{Bu}_3\text{MeNTf}_2\text{N}$, (e) 80 wt. % PVC-20 wt. % $\text{Bu}_3\text{MeNTf}_2\text{N}$ between 550 to 850 cm^{-1} region.

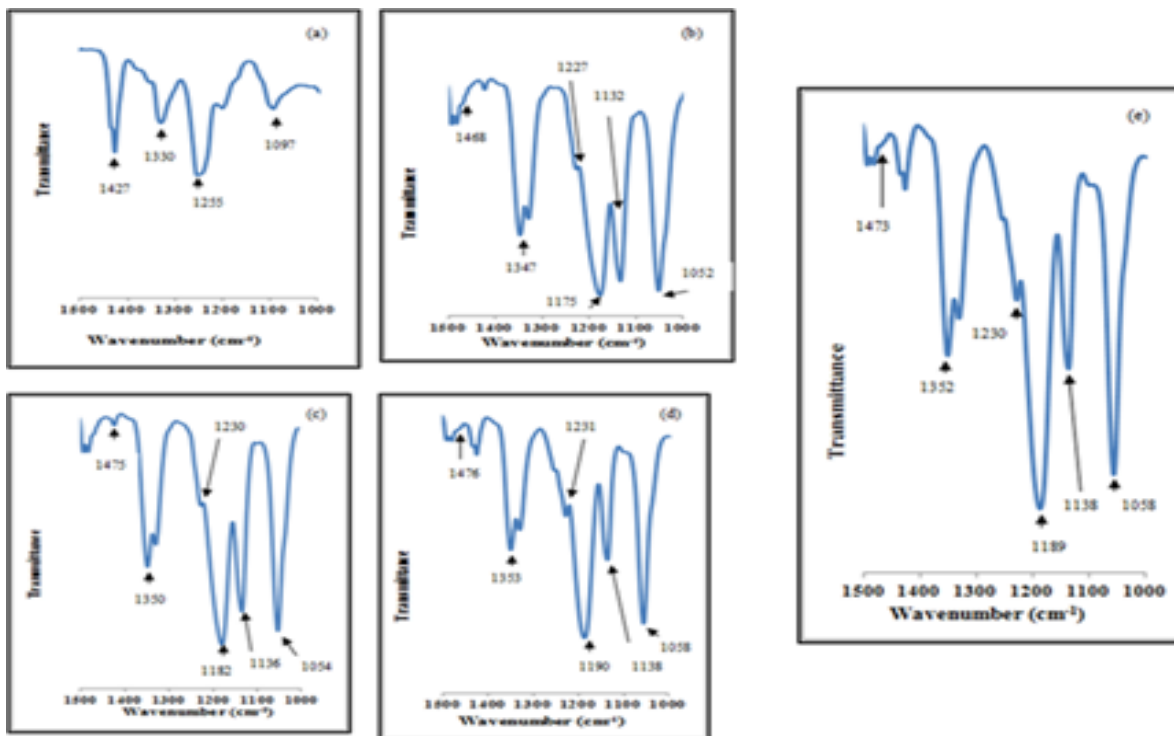


Figure-3. Infrared spectrum of (a) Pure PVC, (b) Pure $\text{Bu}_3\text{MeNTf}_2\text{N}$, (c) 20 wt. % PVC-80 wt. % $\text{Bu}_3\text{MeNTf}_2\text{N}$, (d) 50 wt. % PVC -50 wt. % $\text{Bu}_3\text{MeNTf}_2\text{N}$, (e) 80 wt. % PVC-20 wt. % $\text{Bu}_3\text{MeNTf}_2\text{N}$ between 1000 to 1500 cm^{-1} region.



www.arnjournals.com

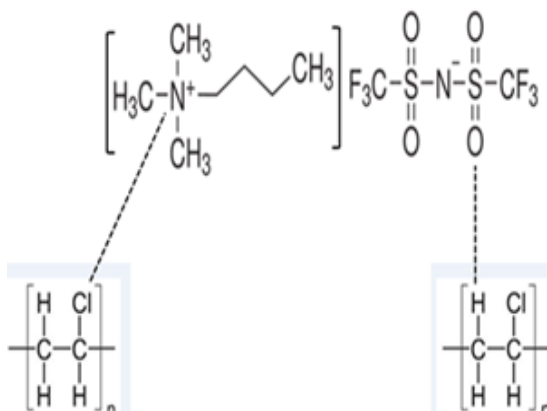


Figure-4. Interaction between $\text{Bu}_3\text{MeNTf}_2\text{N}$ and PVC.

FTIR spectra of $\text{NH}_4\text{CF}_3\text{SO}_3$ - $\text{Bu}_3\text{MeNTf}_2\text{N}$ system

Figure-5 (a)-(e) shows the infrared spectra of the $\text{NH}_4\text{CF}_3\text{SO}_3$ - $\text{Bu}_3\text{MeNTf}_2\text{N}$ system in the region of 900-1100 cm^{-1} . The existence of 'free' triflate ion of the salt is shown at 1028 cm^{-1} , while that in a $\text{NH}_4\text{CF}_3\text{SO}_3$ - $\text{Bu}_3\text{MeNTf}_2\text{N}$ system this band shifted to 1032 cm^{-1} with higher intensity when the ratio of salt to $\text{Bu}_3\text{MeNTf}_2\text{N}$ is

1:1. Its intensity is however low when $\text{Bu}_3\text{MeNTf}_2\text{N}$ concentration is high. This interaction shows that the presence of $\text{Bu}_3\text{MeNTf}_2\text{N}$ increases the number of 'free' ions of the salt as a result of its dissociation by $\text{Bu}_3\text{MeNTf}_2\text{N}$, and this happens up to a certain concentration of $\text{Bu}_3\text{MeNTf}_2\text{N}$. This interaction is consistent with that reported in Figure-1(ii) (a)-(i) presented earlier. The peak due to $\text{Bu}_3\text{MeNTf}_2\text{N}$ at 1053 cm^{-1} meanwhile has disappeared in the spectra of $\text{NH}_4\text{CF}_3\text{SO}_3$ - $\text{Bu}_3\text{MeNTf}_2\text{N}$, which is consistent with that reported in Figure-1(ii) (a)-(i). The possible evidence to prove the interaction between $\text{NH}_4\text{CF}_3\text{SO}_3$ and $\text{Bu}_3\text{MeNTf}_2\text{N}$ is observed at 1053 cm^{-1} . This characteristic peak which assigned as S-N-S asymmetric stretching mode of $\text{Bu}_3\text{MeNTf}_2\text{N}$ exhibits upward shift from 1053 cm^{-1} to 1060 cm^{-1} . In terms of peak intensity, it increases. The changes in shift, shape and intensity have divulged that there is interaction between $\text{NH}_4\text{CF}_3\text{SO}_3$ and $\text{Bu}_3\text{MeNTf}_2\text{N}$ despite them having same anions. The interaction between $\text{NH}_4\text{CF}_3\text{SO}_3$ and $\text{Bu}_3\text{MeNTf}_2\text{N}$ may be represented as shown in Figure-6.

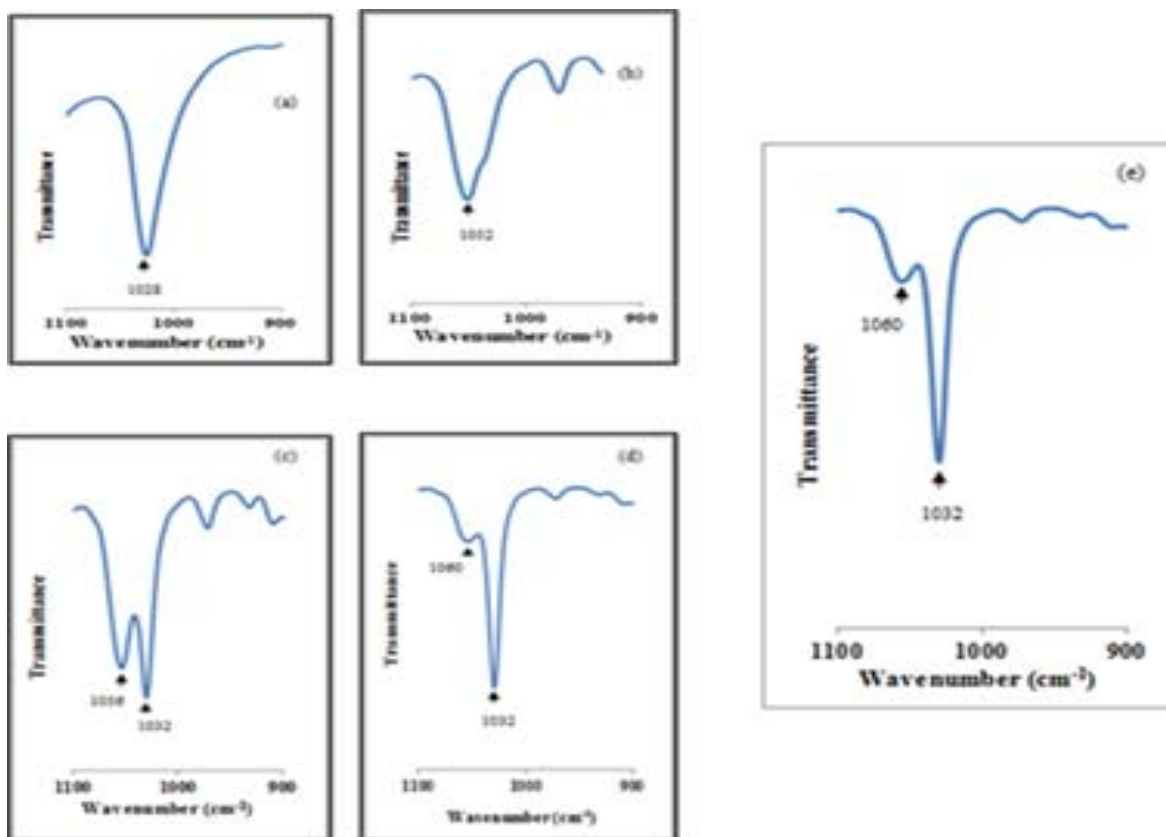


Figure-5. Infrared spectrum of (a) Pure $\text{NH}_4\text{CF}_3\text{SO}_3$ (b) Pure $\text{Bu}_3\text{MeNTf}_2\text{N}$, (c) 20 wt. % $\text{NH}_4\text{CF}_3\text{SO}_3$ -80 wt. % $\text{Bu}_3\text{MeNTf}_2\text{N}$, (d) 50 wt. % $\text{NH}_4\text{CF}_3\text{SO}_3$ -50 wt. % $\text{Bu}_3\text{MeNTf}_2\text{N}$, (e) 80 wt. % $\text{NH}_4\text{CF}_3\text{SO}_3$ -20 wt. % $\text{Bu}_3\text{MeNTf}_2\text{N}$ between 900 to 1100 cm^{-1} region.



www.arpnjournals.com

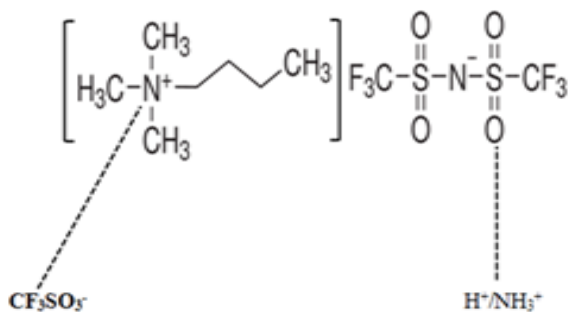


Figure-6. Interaction between $\text{NH}_4\text{CF}_3\text{SO}_3$ and $\text{Bu}_3\text{MeNTf}_2\text{N}$.

CONCLUSIONS

The interaction that exists between the components of PVC- $\text{NH}_4\text{CF}_3\text{SO}_3$ with ionic liquid ($\text{Bu}_3\text{MeNTf}_2\text{N}$) were manifested experimentally in FTIR study as shifts in wave numbers, splitting of the internal vibrational modes and alteration in band shape and intensities. FTIR studies showed that upon addition of ionic liquid, some interactions occurred in the PVC based polymer electrolyte. FTIR spectroscopy provides an insight into the possible interactions between $\text{NH}_4\text{CF}_3\text{SO}_3$, ionic liquid and the host polymer and clearly explains the conduction mechanism in the polymer electrolytes.

REFERENCES

- [1] K. Xu. 2004. Nonaqueous liquid electrolytes for lithium-based rechargeable batteries. *Chemical Reviews*. 104(10): 4303-4418.
- [2] M. Armand. 1989. Charge transfer at polymer electrolytes. *Faraday Discussions of the Chemical Society*. 88: 65-76.
- [3] Gray F. M. 1991. *Solid polymer electrolytes: Fundamentals and technological applications*. 1st Ed. Wiley-VCH. New York, USA. 1991.
- [4] J. R. MacCallum, M. J. Smith and C. A. Vincent. 1984. The effects of radiation-induced crosslinking on the conductance of $\text{LiClO}_4 \cdot \text{PEO}$ electrolytes. *Solid State Ionics*. 11(4): 307-312.
- [5] T. Tatsuma, M. Taguchi, M. Iwaku, T. Sotomura and N. Oyama. 1999. Inhibition effects of polyacrylonitrile gel electrolytes on lithium dendrite formation. *Journal of Electroanalytical Chemistry*. 472(2): 142-146.
- [6] A. Ghosh and P. Kofinas. 2008. Nanostructured block copolymer dry electrolyte. *Journal of the Electrochemical Society*. 155(6): A428-A431.
- [7] T. Uno, S. Kawaguchi, M. Kubo and T. Itoh. 2008. Ionic conductivity and thermal property of solid hybrid polymer electrolyte composed of oligo (ethylene oxide) unit and butyrolactone unit. *Journal of Power Sources*. 178(2): 716-722.
- [8] H. M. J. C. Pitawala, M. A. K. L. Dissanayake, V. A. Seneviratne, B. E. Mellander and I. Albinson. 2008. Effect of plasticizers (EC or PC) on the ionic conductivity and thermal properties of the (PEO) $9\text{LiTf} \cdot \text{Al}_2\text{O}_3$ nanocomposite polymer electrolyte system. *Journal of Solid State Electrochemistry*. 12 (7-8): 783-789.
- [9] Y. W. Chen-Yang, Y. L. Wang, Y. T. Chen, Y. K. Li, H. C. Chen and H. Y. Chiu. 2008. Influence of silica aerogel on the properties of polyethylene oxide-based nanocomposite polymer electrolytes for lithium battery. *Journal of Power Sources*. 182(1): 340-348.
- [10] A. M. Stephan and K. S. Nahm. 2006. Review on composite polymer electrolytes for lithium batteries. *Polymer*. 47(16): 5952-5964.
- [11] J. H. Shin, W. A. Henderson and S. Passerini. 2005. PEO-based polymer electrolytes with ionic liquids and their use in lithium metal-polymer electrolyte batteries. *Journal of the Electrochemical Society*. 152(5): A978-A983.
- [12] J. H. Shin, W. A. Henderson and S. Passerini. 2005. An elegant fix for polymer electrolytes. *Electrochemical and Solid-State Letters*. 8(2): A125-A127.
- [13] J. H. Shin, W. A. Henderson and S. Passerini. 2003. Ionic liquids to the rescue? Overcoming the ionic conductivity limitations of polymer electrolytes. *Electrochemistry Communications*. 5(12): 1016-1020.
- [14] Y. S. Fung and R. Q. Zhou. 1999. Room temperature molten salt as medium for lithium battery. *Journal of Power Sources*. 81: 891-895.
- [15] R. C. Agrawal and G. P. Pandey. 2008. Solid polymer electrolytes: Materials designing and all-solid-state battery applications: An overview. *Journal of Physics D: Applied Physics*. 41(22): 1-18.
- [16] H. Nakajima and H. Ohno. 2005. Preparation of thermally stable polymer electrolytes from imidazolium-type ionic liquid derivatives. *Polymer*. 46(25): 11499-11504.
- [17] M. Morita, T. Shirai, N. Yoshimoto and M. Ishikawa. 2005. Ionic conductance behavior of polymeric gel electrolyte containing ionic liquid mixed with magnesium salt. *Journal of Power Sources*. 139(1): 351-355.
- [18] P. Bonhote, A. P. Dias, N. Papageorgiou, K. Kalyanasundaram and M. Grätzel. 1996.



Hydrophobic, highly conductive ambient-temperature molten salts. *Inorganic Chemistry*. 35(5): 1168-1178.

- [19] W. Lu, K. Henry, C. Turchi and J. Pellegrino. 2008. Incorporating ionic liquid electrolytes into polymer gels for solid-state ultracapacitors. *Journal of the Electrochemical Society*. 155(5): A361-A367.
- [20] N. Terasawa, I. Takeuchi, K. Mukai and K. Asaka. 2010. The effects of Li salts on the performance of a polymer actuator based on single-walled carbon nanotube-ionic liquid gel. *Polymer*. 51(15): 3372-3376.
- [21] H. Cheng, C. Zhu, B. Huang, M. Lu and Y. Yang. 2007. Synthesis and electrochemical characterization of PEO-based polymer electrolytes with room temperature ionic liquids. *Electrochimica Acta*. 52(19): 5789-5794.
- [22] J. Sun, D. R. MacFarlane and M. Forsyth. 2002. Lithium polyelectrolyte-ionic liquid systems. *Solid State Ionics*. 147(3): 333-339.
- [23] P. E. Stallworth, J. J. Fontanella, M. C. Wintersgill, C. D. Scheidler, J. J. Immel, S. G. Greenbaum and A. S. Gozdz. 1999. NMR, DSC and high pressure electrical conductivity studies of liquid and hybrid electrolytes. *Journal of Power Sources*. 81: 739-747.
- [24] J. M. Tarascon and M. Armand. 2001. Issues and challenges facing rechargeable lithium batteries. *Nature*. 414(6861): 359-367.
- [25] H. Matsumoto, T. Matsuda and Y. Miyazaki. 2000. Room temperature molten salts based on trialkylsulfonium cations and bis (trifluoromethylsulfonyl) imide. *Chemistry Letters*. 29(12): 1430-1431.
- [26] K. Tsunashima and M. Sugiya. 2007. Physical and electrochemical properties of low-viscosity phosphonium ionic liquids as potential electrolytes. *Electrochemistry Communications*. 9(9): 2353-2358.
- [27] S. Ramesh, K. H. Leen, K. Kumutha and A. K. Arof. 2007. FTIR studies of PVC/PMMA blend based polymer electrolytes. *Spectrochimica Acta Part A: Molecular and Biomolecular Spectroscopy*. 66(4): 1237-1242.
- [28] C. W. Liew, S. Ramesh and A. K. Arof. 2014. Good prospect of ionic liquid based-poly (vinyl alcohol) polymer electrolytes for supercapacitors with excellent electrical, electrochemical and thermal properties. *International Journal of Hydrogen Energy*. 39(6): 2953-2963.